A High-Precision Ultra Wideband Impulse Radio Physical Layer Model for Network Simulation

Jérôme Rousselot and Jean-Dominique Decotignie
CSEM
Systems Engineering
Real-Time Software and Networking
Jaquet-Droz 1
Neuchâtel, CH-2007 Switzerland
jerome.rousselot@csem.ch

ABSTRACT

Ultra Wideband Impulse Radio (UWB-IR) technology has received a lot of attention from the radio engineering community during the past few years. It features a number of attractive characteristics for wireless sensor networks, among which an ultra low power consumption, a strong robustness to interference and a high accuracy ranging capability.

Unfortunately, its time-based nature makes it difficult to model in a network simulator. Although some mathematical models have been proposed, all of them are limited to a particular modulation type, a specific receiver architecture and often to a channel model. This situation has slowed down the development of communication protocols specifically designed for these radios.

This paper presents a novel symbol-level simulator for UWB-IR which can accurately model pathloss, large-scale fading, small-scale fading and collisions. This physical layer is used to implement a model of an IEEE 802.15.4A UWB-IR radio transceiver based on energy detection.

To the knowledge of the authors, this is the first network simulation model of IEEE 802.15.4A UWB-IR radios, the first model of an energy-detection receiver and more generally the first network simulation model of symbol-level UWB-IR. It offers several channel models of various complexity, so that exploratory simulations can be run quickly and high precision results can be generated when desired. This simulation model allows to evaluate precisely the bit error rate and in particular the impact of collisions, a major cause of energy waste at the medium access control level.

Categories and Subject Descriptors

C.2.1 [**Computer-Communication Networks**]: Network Architecture and Design—*Wireless Communications*; I.6.7 [**Simulation and Modeling**]: Simulation Support Systems

General Terms

Algorithms, Performance, Design, Standardization, Measurement

Keywords

Ultra Wideband, Impulse Radio, Multiple Access Interference, IEEE 802.15.4A, Simulation, Modeling

OMNeT++ 2009, Rome, Italy.

1. INTRODUCTION

Ultra Wideband [28] is a radio technology defined by the FCC [13] as any signal whose bandwidth is larger than 0.2 times its center frequency, or larger than 500 MHz. Regulations allow the unlicensed operation of UWB devices on spectrum already allocated for narrow band systems, the strict power limits imposed to UWB preventing interferences with already deployed systems.

Several approaches have been developed to make use of this spectrum; multi-band orthogonal frequency division multiplexing (MB-OFDM UWB) [6], Impulse Radio (UWB-IR) [30], FM-UWB [14]. MB-OFDM has been selected for Wireless USB devices, Impulse Radio has been standardized as an alternative physical layer for wireless sensor networks in the IEEE 802.15.4A standard [2] and FM-UWB is a candidate physical layer for the upcoming IEEE 802.15.6 standard [1].

Among those, Impulse Radio is the most challenging to model in a network simulator. Based on the emission of short impulses in the order of the nanosecond, and using long guard times to protect against Inter Symbol Interference (ISI), this technology makes multi user interference especially problematic to evaluate.

Several analytic models [27, 31, 16, 18] have been developed. To allow this approach, many assumptions have been made, some of which were later invalidated [8]. Due to the current lack of available hardware, these analytic models cannot be easily validated experimentally. The existing models are also often restricted to a combination of a specific modulation, a specific receiver, and a specific channel model. They are difficult to adapt to other cases (modulation, receiver, channel) because of the assumptions necessary to simplify the computations.

This paper presents and alternative approach. Instead of aiming to obtain an analytic model, it models the packets at the pulse level. The modulation, the propagation and the reception are clearly separated, allowing to evalu-

Digital Object Identifier: 10.4108/ICST.SIMUTOOLS2009.5628
http://dx.doi.org/10.4108/ICST.SIMUTOOLS2009.5628

ate several receiver designs for the same modulation type. The radio power consumption is easily obtained by monitoring the time spent by the radio in each possible state. A complete implementation of the IEEE 802.15.4A standard is described, using the official channel models as specified in [20].

This paper is structured as follows. Section 2 gives a brief overview of the IEEE 802.15.4A UWB Phy layer, section 3 discusses related work, section 4 presents a detailed UWB-IR symbol-level simulation model and its use to study the IEEE 802.15.4A UWB Phy layer, section 5 gives implementation details, section 6 presents some simulation results and section 7 concludes the paper.

2. THE IEEE 802.15.4A STANDARD

The IEEE 802.15.4 standard [3] defines physical and medium access control layers for wireless sensor networks. The IEEE 802.15.4A working group [2] was created to develop an alternative physical layer that would provide communications and high precision ranging. The standard consists of two physical layers: an ultra wideband impulse radio layer and a chirp-spread spectrum layer.

2.1 Burst Position Modulation

The IEEE 802.15.4A UWB Phy layer uses a *Burst Position Modulation* (BPM) scheme. Short impulses are sent consecutively to form a burst, and the time position of this burst in the symbol codes the symbol value (0 or 1). The number of pulses per burst and the pulse duration can take several possible values ; in this work, only the values of the mandatory mode, 2 ns per pulse and 16 pulses per burst were considered.

Each symbol codes one data bit value through the burst time position and one error correction bit value in the burst polarity. This last value may not be demodulated by the receiver, but must be present in the signal. Each symbol is divided into four equal time intervals (each of 256.4 ns in the mandatory mode), as shown on Figure 1. The first and third time intervals are further subdivided into time hopping positions (there are eight such positions in the mandatory mode) to smooth the signal's spectrum.

If the burst codes a zero, it is sent during one of the time hopping positions of the first window. Otherwise the burst is sent during one of the time hopping positions of the third window. The second and fourth time intervals are guard times that protect the signal against *Inter Symbol Interference* (ISI): while the signal propagates, multipath components are created by reflections. The guard times are sufficiently large so that the multipath components that could reach the next active time hopping position will be strongly attenuated.

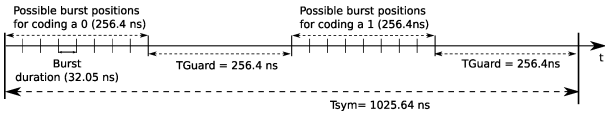

Figure 1: An IEEE 802.15.4A UWB Phy Symbol

2.2 Reception

The very short duration of the pulses makes them difficult to detect. Since there is no carrier signal, the channel is empty most of the time even though a transmission is ongoing. The only part of the signal that can be reliably detected (using a dedicated algorithm) is the *synchronization preamble*, with which all transmissions begin. It consists of a sequence of isolated pulses common to all devices that are part of the network.

Figure 2 shows an IEEE 802.15.4A UWB frame. It starts with the preamble sequence, shown in grey, and it is followed by the Start Frame Delimiter (SFD) and the data payload, both transmitted using Burst Position Modulation.

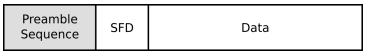

Figure 2: An IEEE 802.15.4A UWB Phy Frame

Several receiver architectures are possible to detect the pulses: the correlation receiver, the energy-detection receiver, the rake receiver... The *correlation* receiver samples the pulse waveform and compares it to a local template. This receiver type can, in addition to detecting the time position of the burst, evaluate its phase (or polarity) and decode an additional error correction bit.

The *energy detection* receiver evaluates the energy on the channel in each time window of the time position modulation and compares these two values to decode the symbol.

More broadly, receiver architectures are divided in two families: *coherent* and *noncoherent*. Coherent receivers (such as the correlation receiver) can demodulate the polarity of the burst while noncoherent receivers (such as energy detection) cannot.

Although the demodulation of the polarity allows to use more sophisticated error correction procedures with coherent receivers, noncoherent receivers have the advantage of simplicity, leading to a lower cost and a lower power consumption. These two characteristics are very important for sensor networks which must operate for years on a single battery and can comprise hundreds of devices.

2.3 Multiple Access Interference

Multiple Access Interference (MAI) is a wireless communication problem that happens when two or more radio signals simultaneously reach a same radio receiver, potentially preventing the message reception. When this is the case, it is said that a *collision* happened. Frame collisions are a well-known cause of energy waste for ultra low power Medium Access Control (MAC) protocols [12, 11].

When simulating narrow band radio systems, the received signal strength can be computed for each frame arriving at the receiver. These values can be used to evaluate the signal to noise ratio during a frame reception, and these values of the signal to noise ratio can be mapped to bit error rates using closed-form analytical expressions (depending on the modulation type).

With UWB-IR systems, the transmitted signal is discontinuous, and thus the received signal strength varies much more frequently. It can be seen on Figure 1 that during most of the IEEE 802.15.4A symbol length (1025.64 ns in the mandatory mode) no signal is transmitted, since there is only one burst of pulses per symbol. This allows the transmitter to be active only during a fraction of the symbol time: 3.1% in the mandatory mode. The receiver, which doesn't know the bit value *a priori*, must listen during both

Digital Object Identifier: 10.4108/ICST.SIMUTOOLS2009.5628
http://dx.doi.org/10.4108/ICST.SIMUTOOLS2009.5628

time windows' time hopping positions and thus must be active during (at least) 6.2% of the symbol in the mandatory mode. This duty-cycling of the transceiver has been studied in [7] to lower the power consumption.

This in-symbol signal duty-cycling offers robustness not only against ISI but also against MAI: since the transmitters are not synchronized, an interfering burst can occur with equal probability at any point during a symbol. There is thus only a probability ${}^{2T_{Burst}}/_{T_{Symbol}}$ that an interfering burst arrives during the time hopping position associated to the opposite bit value of the signal. The probability that this interfering burst arrives during the other time hopping position is also equal to ${}^{2T_{Burst}}/_{T_{Symbol}}$. In both cases, a *pulse collision* happens.

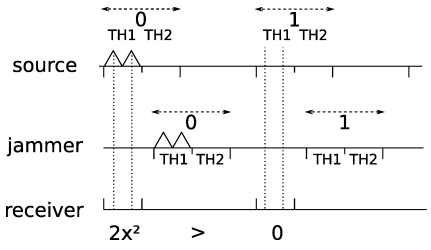

Figure 3: No pulse collision.

When two frames collide, for each symbol of the frame three cases can happen from the receiver's point of view. In the first case, illustrated in Figure 3 (with a two pulses burst and only two time hopping positions for simplicity), the burst of the interfering signal falls between the two positions to code a 0 and to code a 1, and does not have any effect on the receiver.

In the second case, illustrated in Figure 4, the burst of the interfering signal falls somewhere during the burst of the source. This can have a positive effect with an energy-detection receiver.

In the last case, illustrated in Figure 5, the burst of the interfering signal falls during the time position opposite to the value sent by the source. The value demodulated by the receiver depends in this case of the two signals' relative intensities.

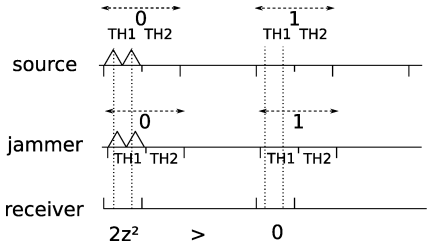

Figure 4: Collision in the same window.

The exact effect of a collision depends on the receiver type. This section focused on an energy-detection receiver that listen only during the two possible burst positions. But some other receivers estimate the channel during the synchronization preamble and listen during larger time windows in order to exploit the multipath components of the signal. In that case, the probability of collision increases. For correlation receivers, a collision of two pulses in the same window

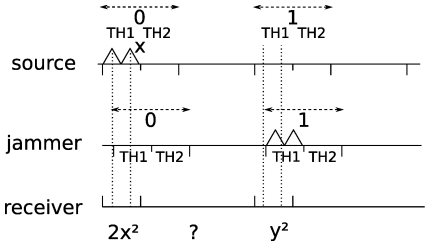

Figure 5: Collision in opposite windows.

makes the pulse waveform more difficult to detect, while for an energy-detection receiver the same collision can improve the demodulation.

2.4 Error Correction

The standard proposes two error correction schemes, a mandatory one and an optional one.

The mandatory scheme is based on a Reed-Solomon code that must be encoded as additional symbols at the end of the packet by all transmitters and which can be demodulated by all receivers.

The optional convolutional code can be encoded by some transmitters and can be demodulated and used by coherent receivers. It is mathematically more complex, but could improve greatly the robustness of the transmissions as it stores one parity bit in the burst polarity of each symbol.

3. RELATED WORK

This section describes several existing models that evaluate the multi user interference in UWB-IR systems.

3.1 The Gaussian Approximation

By assuming that the sum of all interfering signals is a mean-zero Gaussian random process, it is possible [9, 31, 22] to derive the bit error rate as a function of the number of currently active users for a correlation receiver and for an Average White Gaussian Noise (AWGN) channel, for various modulations: Time-Hopping Pulse Position Modulation (TH-PPM), Time-Hopping Phase Shift Keying (TH-PSK) and Direct Sequence Phase Shift Keying (DS-PSK).

This approach is simple and fast, and can be adapted to multipath channels [10]. However, the Gaussian Approximation has been shown [4, 8] to over-estimate the performance. In addition, its adaptation to energy detection receivers is not straightforward.

3.2 Characteristic Function

An alternative to the Gaussian Approximation is to compute characteristic functions (CF) [21]. This approach has been applied to DS and TH PPM and Pulse Amplitude Modulation (PAM), and to AWGN and log-normal fading multipath channels. Here again, only the correlation receiver was considered.

The CF approach, however, requires numerical evaluations of some integrals. The precision of the simulation results depends on the precision with which the integrals are evaluated, and this can greatly slow down the simulations.

3.3 The Pulse Collision Model

Digital Object Identifier: 10.4108/ICST.SIMUTOOLS2009.5628
http://dx.doi.org/10.4108/ICST.SIMUTOOLS2009.5628

In [16], the authors consider that errors are caused by pulse collisions. They evaluate for each symbol the number of possible pulse collisions (depending on the number of currently active transmissions), the probability of each case and the impact on the bit error rate for each case.

This leads to an analytic expression of the bit error rate for correlation receivers in AWGN channels for pulse position modulation and time hopping coding. Unfortunately, it is difficult to introduce multipath channels in the model or to consider energy detection receivers.

3.4 Large Deviations and Importance Sampling

In [18], the authors combine two methods, large deviation and importance sampling, for computing the BER of a coherent rake receiver with a correlation detector, using BPSK modulation and with arbitrary multipath channels between the transmitters and the receiver.

Large deviation is fast but makes the assumption that all interferers are small. Therefore the approach taken by the authors is to use the more computionally intensive method of importance sampling for so-called large interfers, and to use large deviations otherwise.

Unfortunately this work was not adapted to BPM modulation or to non-coherent receivers, and is not currently available for network simulation.

3.5 Cumulative Noise

The only UWB-IR physical layer model for network simulation publicly available today is described in [19]. It considers BPSK modulation and time hopping coding with variable bit rate, and a deterministic channel model without multipath inspired from [15].

It associates an average power level to each packet, computes an average noise level from interfering packets during the reception of a packet, and uses lookup tables to convert this average signal to noise ratio into a bit error rate. The data from the lookup tables are derived from Matlab simulations.

It is difficult to adapt to position modulation or to energy detection receivers since the lookup tables must be regenerated.

3.6 CTU

An analytical framework named CTU [5] aims to evaluate the saturation throughput of MAC protocols for Impulse Radio using pulse position modulation, considering log-normal fading multipath channels.

Its application is restricted to nodes deployed randomly and uniformly on a square region. In addition, this framework requires precise knowledge of the MAC protocol: the probability of being in one of the protocol's states (the stationary distribution) must be known. This is difficult to evaluate for today's sophisticated MAC protocols.

3.7 Conclusion

The problem of modeling MAI for UWB-IR systems has been studied extensively and using various approaches. However, they are often restricted to the correlation receiver, some have not been or can not be adapted to pulse position modulation (which is necessary to model the IEEE 802.15.4A UWB standard), and some are restricted to simple channel models that do not account for multipath propagation.

Among all the approaches discussed above, only one was implemented in a network simulator.

4. PROPOSAL

This section describes a flexible ultra wideband simulation model based on the Omnet++ discrete event simulation engine [29] and on the MiXiM simulation framework [17]. The MiXiM simulation framework is a library of simulation models for wireless and mobile networks. It is straightforward to adapt to novel communication channels and provides software components that facilitate modeling detailed physical phenomena. This allows to focus on the physical processes instead of introducing novel concepts in the simulator as was done in [19] with NS-2.

Instead of implementing an analytical closed-form model of bit error rate, the approach taken here is to model every single pulse of each symbol. The channel model generates multipath components, and the receiver builds a list of all interfering signals that reaches it during the reception of a packet. The receiver computes the probability of successfully decoding each symbol as a function of all pulses present in the two modulation positions of the symbol.

This information is then used to compute the demodulation error probability for each symbol. This probability depends on the receiver architecture. This work considers an energy detection receiver, but other architectures could be implemented as well.

In the particular case of the energy detector, two types of interference can happen: *negative interference* when the interfering pulses fall in the window coding the opposite value (e.g. coding a 1 when the transmitter sent a 0) and *positive interference* when the interfering pulses fall in the window in which the pulses of the transmitted signal have been sent.

4.1 Assumptions

Our current implementation makes the following assumptions: no clock drift, channel coherence time larger than packet duration, no interference from other systems, triangular pulse shapes, no time hopping, uniform random data bits, no error correction, noncoherent energy-detection receiver and simple threshold-based synchronization logic.

- No clock drift: since each system has its own clock, clock drift is unavoidable. The synchronization preamble of a packet allows the receiver to synchronize on the transmitter's clock. Without clock drift, after synchronizing on the preamble, the synchronization remains accurate for the whole packet duration: the energy detection receiver always samples energy perfectly at the peak of the considered pulse. In practice, techniques such as pulse tracking at the circuit level and relative clock drift learning at the MAC level allow to compensate the effect of clock drift.

- The channel coherence time is larger than the packet duration: the parameters characterizing the channel are randomly generated at the beginning of the packet reception, and are not modified during the reception. New channel parameters are generated at each packet arrival.

- Interference from other UWB systems such as MB-OFDM-UWB or FM-UWB, or from narrow band systems such as IEEE 802.11, are not taken into account.

Digital Object Identifier: 10.4108/ICST.SIMUTOOLS2009.5628
http://dx.doi.org/10.4108/ICST.SIMUTOOLS2009.5628

This could be added at a later time thanks to the architecture of the MiXiM simulation framework.

- Triangular pulses: this simplifies the storage of the pulse waveform thanks to linear interpolation, and is also realistic because such pulses are easy to generate. More sophisticated waveforms such as the Gaussian monocycle could be easily modeled similarly, except that more points should be stored.
- No time hopping: the bursts are always located in the first time hopping position of a signal that code either a zero or a one. It is assumed that since the nodes are not synchronized at the symbol level, the statistical bit error rate is the same with and without time hopping (if the number of tranmissions is large enough).
- No error correction: Since the standard does not mandate the decoding of any of the schemes, the current implementation is close to the standard even though it does not yet generate the Reed-Solomon error correction bits at the end of the packets.
- Random bit values: the MAC layer computes the total packet size and generates as many bit values with a uniform random variable.
- Energy detection receiver: this architecture was chosen because it has not been studied as extensively as the correlation receiver and because of its low complexity. This property make it interesting for sensor networks, despite its lower performance.
- Synchronization: since UWB-IR is a carrierless transmission, the signal is difficult to detect. Interferences during synchronization can cause misdetection. A randomized approach was taken in [19]. Here, the radio synchronizes on the first synchronization preamble beginning if this signal is higher than some threshold. The interference from other ongoing transmissions is not yet modeled.

4.2 Transmitter

The generated signal implements the Burst Position Modulation of the standard, using the mandatory mode. Power consumption estimates are taken from [25], and pulses have a triangular shape. This pulse shape has the advantages of being simple to generate in real hardware implementations and of being simple to represent in memory and to manipulate, as only three values must be stored per pulse to mark the start, the end and the peak of the pulse (the other values are linearly interpolated). The synchronization preamble used has the default size of 71.5 µs.

The Reed-Solomon error correction code that is required for compliant transmitters has not yet been implemented in this model. Since the use of this information is optional at the receiver, the simulator's results remain valid with regard to the IEEE 802.15.4A standard.

4.3 Channel

Most channel models specified by the IEEE 802.15.4A working group [20] have been implemented: Residential Line of Sight (LOS) CM1, Residential Non Line of Sight (NLOS) CM2, Indoor office LOS CM3, Outdoor LOS CM5 and NLOS CM6 and Open outdoor NLOS CM7.

They are based on a modified Saleh-Valenzuelah channel model [26]: for each pulse of each burst, multipaths components are generated according to a stochastic process. The channel is supposed coherent for the duration of the packet. Figure 6 illustrates this model, with the initial pulse shown in grey and the smaller pulses caused by the channel shown in white. The number of clusters, the amplitudes of the echoes and the number of pulses in each cluster are all determined using stochastic models.

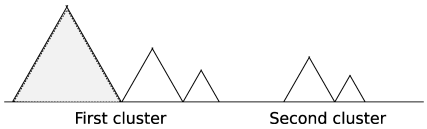

Figure 6: A pulse and its echoes as specified in the IEEE 802.15.4A channel model.

In addition, the simpler and faster stochastic channel model proposed by Ghassemzadeh [15] has also been implemented. This allows to run simulations faster while still keeping a good degree of precision.

For all models, several parameters that describe the channel are generated according to random variables (Poisson for the IEEE models and truncated Gaussians for the Ghassemzadeh model), for each packet.

4.4 Receiver

An energy-detection receiver has been implemented. The current synchronization logic is very simple. It evaluates the mean power level of the synchronization preamble and assumes that the synchronization is successful if this value is higher than some threshold. Currently, the interferences of the other ongoing transmissions on the synchronization preamble are not considered.

For each data symbol, it considers the two burst positions coding respectively a zero and a one. The receiver does not attempt to collect the energy of the multipath components.

At each pulse peak position in the burst, the receiver samples the energy on the channel and squares it. The sums of all squares for each window are compared, and the bit value associated to the window with the highest energy level is decoded.

If the two energy values are too close to each other, a random bit value is generated. The threshold for this case is set at run-time by the simulation user. If there are interfering signals, they are taken into account when sampling the channel, and in addition, the thermal noise in the receiver is also modeled.

In the current implementation, a packet is discarded if it has at least one bit error.

The estimate of the receiver's power consumption is taken from a correlation receiver as described in [24, 7]. As correlation receivers are more complex, the power consumption of energy-detection receivers should be below that value.

5. IMPLEMENTATION DETAILS

Contrarily to NS-2 [19], the MiXiM simulation framework provides good foundations for implementing such a low-level model. More information on this framework can be found in [17].

Digital Object Identifier: 10.4108/ICST.SIMUTOOLS2009.5628
http://dx.doi.org/10.4108/ICST.SIMUTOOLS2009.5628

5.1 Physical Layer

An *UWBIRPhyLayer* class was introduced. It instantiates the channel model and the decider chosen by the user, and initializes the radio model.

5.2 Radio Model

MiXiM provides a detailed four states radio model that allows to take into account transition states: *Idle*, *Reception*, *Transmission* and *Switching*.

A fifth radio state, *Synchronization*, that precedes *Reception*, was added. The evaluation of the radio power consumption is done in an *UWBIRRadio* subclass of *Radio*, by counting the time spent in each state of the radio.

5.3 Signal and Packet Structure

The data to send is encoded in a *TimeMapping* object as provided by the MiXiM framework. Each pulse is stored with three points, marking the beginning, the peak and the end of the triangular pulse. The amplitude of the pulse at any point in time is computed by linear interpolation.

Since the decider demodulates the signal, it needs the original bit values to evaluate the bit error rate. In the current implementation, they are generated randomly at the MAC layer, and stored in a *UWBIRMacPkt* Omnet++ message.

5.4 Synchronization

The synchronization preamble of the IEEE 802.15.4A is generated and stored at the beginning of the TimeMapping object that represents the signal.

The synchronization logic is implemented in the *bool UWBIREnergyDetectionDeciderV2 ::attemptSync(ConstMappingIterator* mIt)* method. It returns *true* if the synchronization was successful, and *false* otherwise. Other synchronization algorithms can be implemented by subclassing the decider and simply overloading this method.

6. EVALUATION

6.1 Channel Models

Figure 7 shows the Bit Error Rate as a function of the distance between a source and a receiver. The receiver uses energy detection with a 3 dB sensitivity. The source sends 100 packets of 80 bits each, and the simulation is run three times for each combination of distance and channel model. Ten points are considered between 1 and 10 meters and nine points from 20 to 100 meters.

Four channels models are evaluated: the Ghassemzadeh Line of Sight and Non Line of Sight models, and the IEEE 802.15.4A residential LOS (CM1) and residential NLOS (CM2) models. The results for the Ghassemzadeh LOS can not be seen on the figure since all bit values were correctly demodulated and thus the BER is equal to zero. Similarly, the CM1 (LOS) model shows a low BER for all distances. The CM2 (NLOS) model transitions abruptly from a low BER between 0.001 and 0.01 around 7 meters to its peak of 0.5 starting at 10 meters. The Ghassemzadeh NLOS shows a similar trend, albeit following a smoother line and with a slightly better performance.

The good results obtained with both LOS channels highlight the problem of their validity range. For instance, the CM1 model is based on measurements covering a range between 3 and 28 meters. More generally, an increase of distance usually decreases the probability of a LOS link when deploying radio systems. Thus, NLOS channel models should be preferred.

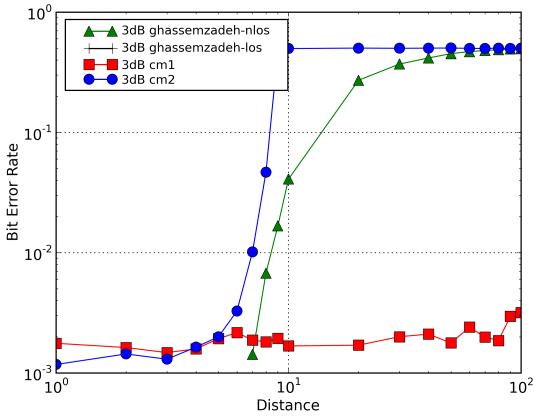

Figure 7: Bit Error Rate as a function of the link distance with channel models Ghassemzadeh LOS, Ghassemzadeh NLOS and IEEE 802.15.4A CM1 (residential LOS) and CM2 (residential NLOS) for a 3dB receiver sensitivity.

6.2 Receiver Sensitivity

The receiver modeled in this work can demodulate a bit value if the difference between the energy in the first time window and the energy in the second time window is larger than a threshold.

Figure 8 shows the bit error rate as a function of the distance between the sender and the receiver on a bilogarithmic graph, for three receiver configurations: the sensitivity was set to 1, 3 and 10 dB. The simulations were run for 19 different distances, and for each distance three runs were made to avoid bias from the pseudo random number generators. During each run, the sender transmits 100 packets of 80 bits each. Thus for each considered distance, 24000 bits values are randomly generated, time modulated and sent to the receiver. The channel model used is Ghassemzadeh NLOS.

As expected, the performance increases with a higher sensitivity. However, a high sensitivity decreases the robustness of the system in presence of interferers (UWB or narrowband), an effect that cannot be seen in the figure.

6.3 Multiple Access Interference

Figure 9 illustrates the effect on bit error rate of simultaneous transmissions using boxplots and logarithmic axises. The receiver is placed at the center of a square with a length of 20 meters, and all transmitters are placed randomly on this square. During each run, each transmitter sends continuously 250 packets of 10 bytes each. Each case is repeated 15 times to avoid bias because of a particular configuration of the nodes. Thus 300 000 data symbols are demodulated for each number of simultaneous transmissions considered.

When considering only two or three simultaneous transmissions, the median BER is around 5%. This error rate is acceptable, especially for random access protocols, and the final packet error rate would probably benefit from the Reed-Solomon error correction mechanism.

Digital Object Identifier: 10.4108/ICST.SIMUTOOLS2009.5628
http://dx.doi.org/10.4108/ICST.SIMUTOOLS2009.5628

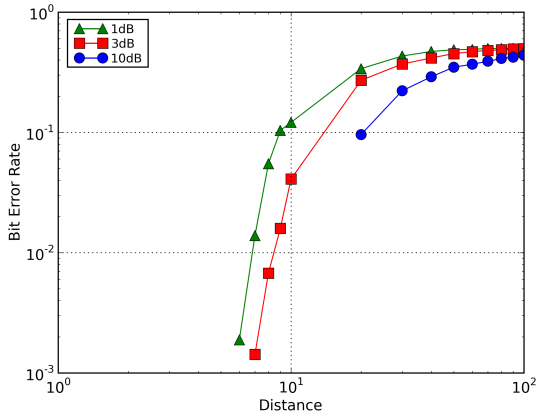

Figure 8: BER as a function of the link distance (Ghassemzadeh NLOS channel model, and various receiver sensitivity settings).

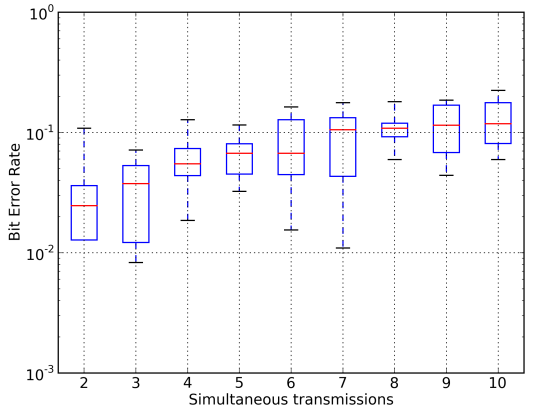

Figure 9: BER as a function of the number of simultaneously transmitting nodes (Ghassemzadeh NLOS channel model, 3 dB receiver sensitivity).

With higher numbers of simultaneous transmissions, the median error rate steadily increases and reaches approximately 10% for the maximum considered number of interferers, 10. The BER degradation is smooth and in all cases, the stochastic channel introduces some level of variability in the results.

6.4 Simulation Performance

The channel model has a major impact on the simulation system's performance. It is recommended to start working with the simpler Ghassemzadeh channel model for exploratory simulations, and to switch to the more complex IEEE 802.15.4A channel models to increase the accuracy of the results when required. For instance, the simulations for figure 7 were seven times slower for the IEEE channel models (on average 15 ms per symbol) than for the Ghassemzadeh channel models (on average 2.2 ms per symbol).

The number of simultaneous transmissions also impacts the computation time. The maximum interference distance should be configured adequately in order to avoid unnecessary computations. The simulation runs for figure 9 suggested a linear relation between the number of simultaneous transmissions and the time to simulate a symbol (from 0.72 ms with two transmitters to 4.98 ms with 9 transmitters).

Note that the performance variation between the two figures is due to the use of different computers.

7. CONCLUSION

This paper presented, to the authors' knowledge, the first generic Ultra Wideband Impulse Radio physical layer model for network simulation. This model works at the symbol level instead of using complex mathematical approximations.

Albeit slower than some of the existing mathematical models, its advantages are numerous. It allows to study all types of receivers, *coherent* as well as *noncoherent,* as illustrated by the energy detector described in this work (many mathematical models favour the correlation receiver). It allows to study the problem of synchronization and in particular the impact of interference on synchronization performace. It also allows to switch between channel models as needed, from simple models to evaluate large parameter spaces to highly detailed models such as the IEEE 802.15.4A channel models when high accuracy is desirable.

In this work, an energy-detection receiver was considered because of its low complexity, making it an ideal choice for sensor networks. The implementation of a correlation receiver would also be interesting for comparison purposes, especially one using the full error correction capabilities of IEEE 802.15.4A.

Further work will focus on the model validation, on enhancements to the synchronization logic and on the implementation of the Reed-Solomon error correction scheme. WideMac [23], a dedicated MAC protocol for UWB-IR will be evaluated in combination with wireless sensor networks routing protocols.

8. REFERENCES

[1] IEEE 802.15 WPAN™ Task Group 6 Body Area Networks (BAN).

[2] IEEE 802.15.4 WPAN Low Data Rate Alternative PHY Layer: http://ww.ieee802.org/15/pub/TG4a.html.

[3] *IEEE Std 802.15.4-2006, IEEE Standard for Information technology-Telecommunications and information exchange between systems-Local and metropolitan area networks-Specific requirements- Part 15.4: Wireless Medium Access Control (MAC) and Physical Layer (PHY) Specifications for Low-Rate Wireless Personal Area Networks (LR-WPANs).*

[4] A. Forouzan, M. Nasiri-Kenari, J. S. Performance Analysis of Time-Hopping Spread-Spectrum Multiple-Access Systems: Uncoded and Coded Schemes. *IEEE Transactions on Wireless Communications 1*, 4 (October 2002), 671–681.

[5] Broustis, I., Vlavianos, A., Krishnamurthy, P., and Krishnamurthy, S. CUT: Capturing Throughput Dependencies in UWB Networks. In *Proc. of the IEEE INFOCOM 2008 Conference* (2008).

[6] Chou, J. d. P. P., Shankar, S., Gaddam, V., Challapali, K., and Chun-Ting. The

Digital Object Identifier: 10.4108/ICST.SIMUTOOLS2009.5628
http://dx.doi.org/10.4108/ICST.SIMUTOOLS2009.5628

MBOA-WiMedia Specification for Ultra Wideband Distributed Networks. *IEEE Communications Magazine 44*, 6 (june 2006), 128–135.

[7] Dolmans, G., Rousseaux, O., Huang, L., Fu, T., Gyselinkx, B., d'Amico, S., Baschirotto, A., Ryckaert, J., and van Poucke, B. UWB Radio Transceivers For Ultra Low Power and Low Data Rate Communications. In *Proc. of the 2007 IEEE International Conference on Ultra-Wideband* (2007).

[8] Durisi, G., and Romano, G. On the Validity of Gaussian Approximation to Characterize the Multiuser capacity of UWB TH PPM. In *IEEE Conference on Ultra Wideband Systems and Technologies* (2002).

[9] Durisi, G., and Romano, G. Performance Evaluation and Comparison of Different Modulation Schemes for UWB Multiaccess Systems. In *Proc. IEEE ICC'03* (2003), pp. 2187–2191.

[10] Efthymoglou, G., Aalo, V., and Helmken, H. Performance analysis of coherent DS-CDMA systems in a Nakagami fading channel with arbitrary parameters. *IEEE Trans. on Vehicular Technology 2*, 46 (1997), 289–297.

[11] Enz, C., El-Hoiydi, A., Decotignie, J.-D., and Peiris, V. WiseNET: an ultralow-power wireless sensor network solution. *Computer 37*, 8 (2004), 62–70.

[12] Estrin, D., Ye, W., and Heidemann, J. Medium Access Control With Coordinated Adaptive Sleeping for Wireless Sensor Networks. *Transactions on Networking 12*, 3 (June 2004), 493–506.

[13] FCC-02-48A1, Revision of Part 15 of the Commission's Rules Regarding Ultra-Wideband Transmission Systems. Tech. rep., Federal Communications Commission, 2002.

[14] Gerrits, J. F. M., Kouwenhoven, M. H. L., van der Meer, P. R., Farserotu, J. R., and Long, J. R. Principles and Limitations of Ultra-Wideband FM Communications Systems. *EURASIP Journal on Applied Signal Processing 3* (2005), 382–396.

[15] Ghassemzadeh, S. Measurement and Modeling of an Ultra-Wide Bandwidth Indoor Channel. *IEEE Transactions on Communications 52*, 10 (2004), 1786.

[16] Giancola, G., and Di Benedetto, M.-G. A novel approach for estimating multi-user interference in impulse radio UWB networks: The pulse collision model. *Signal Processing 86*, 9 (2006), 2185–2197.

[17] Köpke, A., Swigulski, M., Wessel, K., Willkomm, D., Haneveld, P. K., Parker, T., Visser, O., Lichte, H., and Valentin, S. Simulating Wireless and Mobile Networks in OMNeT++: The MiXiM Vision. In *Proceedings of the 1st international conference on Simulation tools and techniques for communications, networks and systems & workshops* (2008).

[18] Merz, R., and Le Boudec, J.-Y. Conditional bit error rate for an impulse radio UWB channel with interfering users. In *Proc. of the IEEE Int. Conf. on Ultra-Wideband (ICUWB'05)* (2005), pp. 130–135.

[19] Merz, R., Le Boudec, J.-Y., and Widmer, J. An Architecture for Wireless Simulation in NS-2 Applied to Impulse-Radio Ultra-Wide Band Networks. In *Proc. of the 10th Communications and Networking Simulation Symposium (CNS07)* (2007).

[20] Molisch, A. F., Balakrishnan, K., Cassioli, D., Chong, C.-C., Emami, S., Fort, A., Karedal, J., Kunisch, J., Schantz, H., Schuster, U., and Siwiak, K. IEEE 802.15.4a channel model - final report. Tech. rep., IEEE 802.15.4 Working Group, 2005.

[21] Niranjayan, S., Nallanathan, A., and Kannan, B. Modeling of Multiple Access Interference and BER Derivation for TH and DS UWB Multiple Access Systems. *IEEE Transactions on Wireless Communications 5*, 10 (2006), 2794–2804.

[22] Pursley, M. Performance Evaluation for Phase-Coded Spread-Spectrum Multiple-Access Communication - Part I: System Analysis. *IEEE Transactions on Communications 30*, 5 (August 1977), 795–799.

[23] Rousselot, J., El-Hoiydi, A., and Decotignie, J.-D. WideMac: a low power and routing friendly MAC protocol for Ultra Wideband sensor networks. In *Proc. of the International Conference on Ultra-Wideband* (2008), pp. 105–108.

[24] Ryckaert, J., Badaroglu, M., De Heyn, V., Van der Plas, G., Nuzzo, P., Baschirotto, A., D'Amico, S., Desset, C., Suys, H., Libois, M., Van Poucke, B., Wambacq, P., and Gyselinckx, B. A 16 mA UWB 3-to-5GHz 20 Mpulses/s Quadrature Analog Correlation Receiver in 0.18micrometer CMOS. In *International Solid-State Circuits Conference* (2006).

[25] Ryckaert, J., Van der Plas, G., De Heyn, V., Desset, C., Vanwijnsberghe, G., Van Poucke, B., and Craninckx, J. A 0.65-to-1.4nJ/burst 3-to-10GHz UWB Digital TX in 90nm CMOS for IEEE 802.15.4a. In *International Solid State Circuits Conference* (2007).

[26] Saleh, A., and Valenzuela, R. A Statistical Model for Indoor Multipath Propagation. *Selected Areas in Communications, IEEE Journal on 5*, 2 (Feb 1987), 128–137.

[27] Scholtz, R. A. Multiple Access with Time-Hopping Impulse Modulation. In *Proc. of the Military Communications Conference (MILCOM'93)* (1993), pp. 447–450.

[28] Scholtz, R. A., Pozar, D. M., and Namgoong, W. Ultra-Wideband Radio. *EURASIP Journal on Applied Signal Processing* (2005), 252–272.

[29] Varga, A. The OMNeT++ Discrete Event Simulation System. In *Proceedings of the European Simulation Multiconference (ESM'2001)* (2001).

[30] Win, M. Z., and Scholtz, R. A. Impulse Radio: How It Works. *IEEE Communications Letters 2*, 2 (February 1998), 36–37.

[31] Win, M. Z., and Scholtz, R. A. Ultra-Wide Bandwidth Time-Hopping Spread-Spectrum Impulse Radio for Wireless Multiple-Access Communications. *IEEE Transactions on Communications 48*, 4 (2000), 679–691.

Digital Object Identifier: 10.4108/ICST.SIMUTOOLS2009.5628
http://dx.doi.org/10.4108/ICST.SIMUTOOLS2009.5628